

See discussions, stats, and author profiles for this publication at: <https://www.researchgate.net/publication/231654227>

Adsorption and Vibrations of α,β -Unsaturated Aldehydes on Pt(111) and Pt–Sn Alloy (111) Surfaces. 3. Adsorption Energy vs Adsorption Strength

ARTICLE *in* THE JOURNAL OF PHYSICAL CHEMISTRY C · DECEMBER 2009

Impact Factor: 4.77 · DOI: 10.1021/jp908353p

CITATIONS

19

READS

27

7 AUTHORS, INCLUDING:



[Jan Haubrich](#)

German Aerospace Center (DLR)

38 PUBLICATIONS 624 CITATIONS

[SEE PROFILE](#)



[C. Becker](#)

Aix-Marseille Université

91 PUBLICATIONS 1,411 CITATIONS

[SEE PROFILE](#)



[Klaus Rainer Wandelt](#)

University of Bonn

436 PUBLICATIONS 8,076 CITATIONS

[SEE PROFILE](#)

Absorption and Vibrations of α,β -Unsaturated Aldehydes on Pt(111) and Pt–Sn Alloy (111) Surfaces. 3. Adsorption Energy vs Adsorption Strength

J. Haubrich,^{*,†} D. Loffreda,[‡] F. Delbecq,[‡] P. Sautet,[‡] Y. Jugnet,[§] C. Becker,^{||} and K. Wandelt[†]

Institut für Physikalische und Theoretische Chemie, Universität Bonn, Wegelerstrasse 12, D-53115 Bonn, Germany; Department of Chemistry and Chemical Biology, Harvard University, 12 Oxford Street, Cambridge Massachusetts 02138, Laboratoire de Chimie, Institut de Chimie de Lyon, Ecole Normale Supérieure de Lyon and CNRS, Université de Lyon, 46 Allée d’Italie, F-69364 Lyon Cedex 07, France, Institut de Recherche sur la Catalyse et l’Environnement de Lyon, UMR5256 CNRS–Université Lyon 1, 2 Avenue A. Einstein, F-69626 Villeurbanne, France, and CINaM–CNRS–UPR 3118, Université de la Méditerranée and Université Paul Cézanne, Campus de Luminy–Case 913, 13288 Marseille Cedex 09, France

Received: August 29, 2009; Revised Manuscript Received: November 29, 2009

Recently we presented high-resolution electron energy loss spectroscopy (HREELS) and temperature-programmed desorption (TPD) studies on the adsorption of prenal (3-methyl-2-butenal) and crotonaldehyde (2-butenal) on Pt(111) and on ultrathin Pt₃Sn/Pt(111) and Pt₂Sn/Pt(111) surface alloys. Vibrational studies employing HREELS have been analyzed with the help of extensive density functional theory (DFT) calculations of the energetic, structural, and vibrational properties of a large set of stable adsorption configurations. We were able to identify various adsorbate structures ranging from low hapticity η^1 -top and η^2 -di σ (CC) to flat η^4 types present in mixed phases below room temperature on these substrates. Completing this study, we now analyze common features and differences between the two molecules on the three surfaces. The key finding is that the adsorption energy turns out to be an unsatisfying measure of the interaction strength of such complex molecules on surfaces. For several identified structures lower desorption temperatures and smaller adsorption energies from DFT corroborated a weaker adsorption strength; however, vibrational and geometric properties obtained consistently from experiments and theory pointed to similarly strong molecule–surface bonding. We will show here that this phenomenon can only be rationalized by clearly differentiating between adsorption energy and interaction energy. Since the adsorption process includes significant relaxations of surface metal atoms and adsorbed molecules to optimize their covalent interactions, there is a deviation between the adsorption strength, measured by the interaction energy, and the final adsorption energy where the endothermic energetic costs of both relaxation processes have to be taken into account. Calculating these properties from DFT, we can show that adsorption energies may indeed decrease while the overall interaction energy of a molecule with a surface can, nonetheless, increase. The adsorption energy is hence not a good, unambiguous measure of molecule–surface interactions.

1. Introduction

One of the major challenges in chemistry is the design of efficient and environmentally benign catalysts for large-scale applications. For that purpose, it is necessary to develop a thorough understanding of the chemical reactions as well as the effects of the catalyst at the atomic scale. The characterization of new materials of potential use in catalytic processes is, hence, a prerequisite to obtain the necessary knowledge for a rational design of advanced catalysts. The bonding of the reactants, reaction intermediates, and products to the catalyst is a major factor determining the energetics of the reaction pathway, and therefore the reactivity. Ideally one wants the reactants to bind selectively only to the active sites.

The α,β -unsaturated aldehydes are important reactants for fine chemicals production in the selective hydrogenation to α,β -unsaturated alcohols.^{1–3} Catalysts are employed in the process since the thermodynamically favored reaction pathway leads

primarily to reduction of the C=C double bond forming saturated aldehydes or even alkanes instead of the desired α,β -unsaturated alcohols, which are obtained by selective hydrogenation of the C=O bond under kinetic control.^{4,5} Alloying Pt catalysts with electropositive metals such as Sn or Fe gives an enhanced selectivity for α,β -unsaturated alcohols.^{6–10}

To contribute to a deeper understanding of the catalytic properties of these materials, we have chosen to study the behavior of crotonaldehyde (2-butenal) and prenal (3-methyl-2-but-en-1-al), two prototypes of reactants, on two ultrathin Pt–Sn alloys in comparison to a pure Pt(111) substrate. Specifically we focus on the interaction of the molecules with the substrates that determine the initial state of the reactants, using a combination of experiments and simulations. Usually the adsorption energy is used as a measure of the bonding strength on catalyst surfaces. Many examples can be found in the literature that show an inherent correlation between adsorption energy and bond strength, which can be shown particularly clearly by employing vibrational spectroscopies (see for instance refs 11–14 and therein). Furthermore the adsorption energy can be used in a purely thermodynamic picture as a crude measure for the ability of a catalyst to activate molecules.¹⁵ The relation is, however, nonmonotonic, with an optimum molecular

* Corresponding author. Fax: +49 228 73 2515. E-mail: janh@pc.uni-bonn.de.

† Universität Bonn and Harvard University.

‡ Ecole Normale Supérieure de Lyon and CNRS, Université de Lyon.

§ UMR5256 CNRS–Université Lyon 1.

|| Université de la Méditerranée and Université Paul Cézanne.

adsorption energy for the catalytic activity expressed in the Sabatier principle.^{16,17}

We employ surface alloying as an important tool to modify and control molecular chemisorption, and our main objective is to understand how the addition of Sn in increasing amounts modifies the adsorption on Pt-based surfaces. For this purpose, we compare the bonding of crotonaldehyde and prenal on Pt(111) with that on two ultrathin surface alloys, Pt₃Sn/Pt(111) and Pt₂Sn/Pt(111), which can be prepared via physical vapor deposition of Sn on Pt(111) and subsequent annealing.^{5,18–23} Both surface alloys are characterized by specific, well-defined superstructures and exhibit Pt ensembles of different sizes. The surface relaxation due to the larger Sn atoms results in protrusions of the latter by 30 and 23 pm above the Pt₃Sn/Pt(111) and Pt₂Sn/Pt(111) surface planes, respectively.¹⁸

Despite the large number of other studies that have been devoted to the adsorption and reactivity of α,β -unsaturated aldehydes such as acrolein, crotonaldehyde, and prenal on Pt-based model catalysts,^{5–10,21,24–34} a consistent understanding of the interaction of α,β -unsaturated aldehydes is missing so far. Several groups have shown in the past that alloying Pt with electropositive promoters such as Fe or Sn^{6,9,10} usually improves the selectivity and activity toward formation of the unsaturated alcohols. Marinelli et al. suggested that alloying with Sn leads to surface sites which activate the C=O group by predominant coordination of the molecules through the aldehydic moiety.^{9,10} However, also other studies exist that found only an increase of the activity upon alloying Pt(111) with Sn and no change in selectivity.⁵

Tin alloyed into Pt surfaces is known to lower the local density of states (LDOS) at the Fermi level¹⁹ and negatively polarizes the neighboring Pt atoms via electron transfer.²⁶ Furthermore this is correlated with an energetic downshift of the Pt d-band center, which, like the intermetallic charge transfer, increases with the surface fraction of Sn and weakens the adsorption of crotonaldehyde and prenal.^{20,26,35,36} Contrary to Sn being often considered as a mere site blocker,²² we recently found that Sn also acts as a preferred adsorption site, in particular since its oxophilic character allows a strong interaction with the aldehydic oxygens.^{20,36}

Janin et al. employed XPS (X-ray photoemission spectroscopy) experiments combined with DFT (density functional theory) total energy calculations to support the determination of potential adsorption configurations.^{21,29} According to their calculations, the η^3 structure of crotonaldehyde is the most stable form on Pt(111), a chemical binding configuration which does not contradict the XPS data. On the Pt–Sn surface alloys, the calculated adsorption energies are weakened, yet the coordination type remains the η^3 structure, but this time with oxygen bonding to Sn atoms. Also a small amount of η^1 -top-OSn structures standing upright on the surface Sn atoms was inferred from the XPS data, which were most abundant on the Pt₂Sn surface alloy. However, a drawback of these studies is that only a limited number of structures on a simplified two-layer surface model was considered, and no core-level shifts were determined from DFT.

Experimental studies of acrolein and crotonaldehyde on Pt(111) using TPD temperature-programmed desorption and RAIRS (reflection–absorption infrared spectroscopy)³⁰ led to the suggestion that the dominating adsorption geometries were flat and the molecules bonded mainly through the C=C double bond in $\text{di}\sigma(\text{CC})$ type configuration.

Following the identification of several η^4 , η^3 , and η^2 adsorption geometries of acrolein on Pt(111), Loffreda et al.³¹ recently

performed theoretical studies on the reaction pathways of the hydrogenation to propanal, propanol, and propenol,^{33,37} finding that the low selectivity of Pt(111) toward the unsaturated alcohol originates from a high desorption energy of propenol rather than from high barriers that would disfavor its formation. On the contrary, these authors showed clearly that the C=O bond is hydrogenated more easily than the C=C one. This underlines the need to identify the adsorption structures on the Pt–Sn model catalysts in order to understand the interaction properties of α,β -unsaturated aldehydes and lays the basis for systematic DFT studies of the changes in the reaction barriers introduced by alloying.

In the first two parts of this series we reported on the identification of the adsorption configurations of prenal²⁰ and crotonaldehyde^{35,36} on Pt(111) and two well-defined Pt–Sn surface alloys, respectively. High-resolution electron energy loss spectroscopy (HREELS) experiments performed for different coverages at low temperature and supported by extensive DFT calculations showed a variety of η^2 -di $\sigma(\text{CC})$, η^3 , η^4 , or vertical η^1 -top structures present in mixed phases on the surface. Surprisingly, we found similarly strong vibrational shifts characteristic of strong binding on Pt(111) and both Pt–Sn surfaces, whereas the DFT adsorption energies and the TPD/TPRS (temperature programmed reaction spectroscopy) characteristics clearly indicated a weak adsorption.

We will here compare the adsorption behavior for both aldehydes on Pt(111) and the two ultrathin Pt–Sn alloys and analyze trends in the geometric and vibrational characteristics of corresponding structures. We will show that the vibrational frequency shifts induced on sensitive vibrations such as $\nu(\text{C}=\text{C})$ or $\nu(\text{C}=\text{O})$ by adsorption and alloying can be understood much better from the changes in the true interaction energies rather than the decrease in the adsorption energies. The relaxation of both the surface and the molecule upon formation of the adsorbate structure³⁸ leads to significant energy costs that, combined with the adsorption energies, allow us to deduce the interaction energies. The interaction energy is, thus, a much better measure of the true bonding strength for the adsorption of multifunctional molecules.

2. Computational Details

The details of the performed experiments and of the DFT analysis have been reported in refs 20 and 36. Therefore, only a concise summary of the computational details is given here.

All DFT computations of the surfaces and adsorbate complexes have been performed with VASP.^{39,40} The generalized gradient approximated (GGA) functional Perdew–Wang 91 (PW91)⁴¹ has been used together with the PAW method⁴² and sufficiently tight convergence criteria for the plane-wave expansion (cutoff of 400 eV). A second-order Methfessel–Paxton smearing was employed together with the Pulay mixing scheme for the electronic states.

Supercells were constructed from four-layer-thick metallic slabs (optimized $r(\text{Pt–Pt}) = 2.82 \text{ \AA}$; experimentally, 2.77 \AA) separated by a five layer thick of vacuum. The molecules were adsorbed on one side of the slab only, and spurious electrostatic interactions between the periodic slabs were, therefore, compensated by a dipole correction scheme.⁴³

In the case of the surface alloys, single alloy layers have been placed over a Pt(111) bulk. We have chosen a medium coverage situation modeled by 3×3 supercells (coverage, 1/9 monolayer) for Pt(111) and Pt₂Sn(111) with 2D Brillouin zone integration on a well-converged $3 \times 3 \times 1$ k-point grids. The Pt₃Sn(111) surface alloy has been modeled from a slightly larger ($2\sqrt{3} \times$

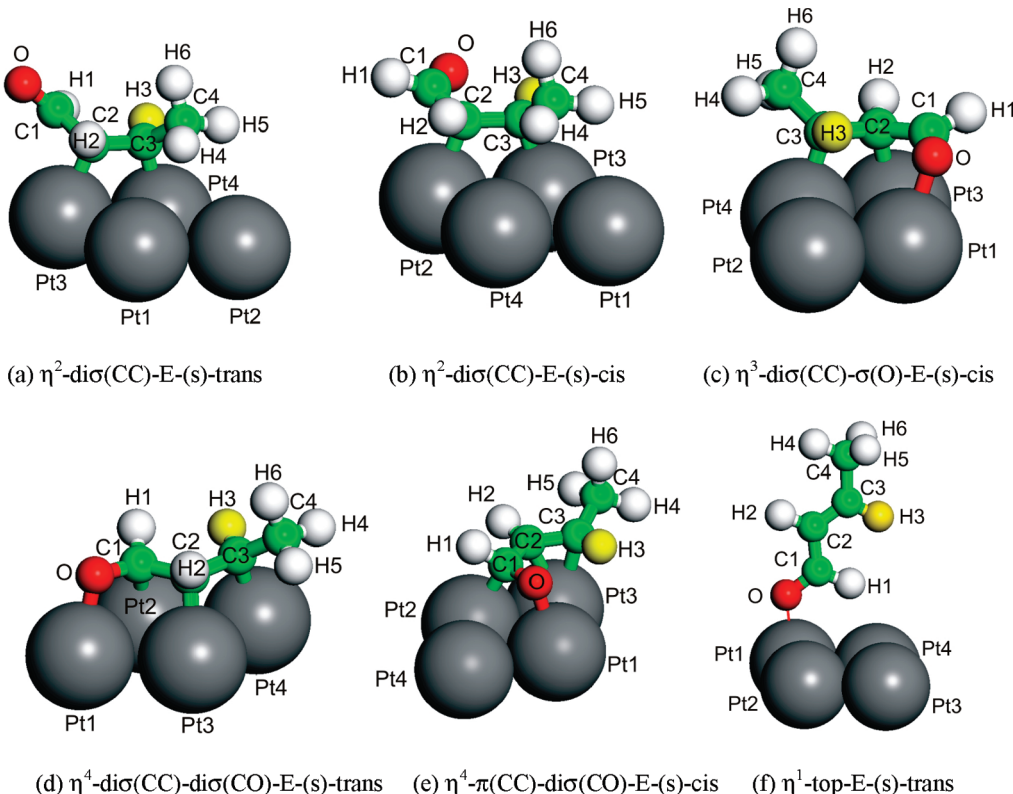


Figure 1. Representative schematic illustration of the discussed bonding configurations of crotonaldehyde on Pt(111). Other α,β -unsaturated aldehydes such as acrolein and prenal form very similar adsorption structures of the same types. Note that hydrogen H3 is highlighted in yellow. Substituting H3 by a methyl (CH_3) substituent leads to the respective prenal configurations and lifts the E/Z isomery on the C=C bond found for crotonaldehyde. On the Pt–Sn surface alloys, the configurations with O–metal coordination bond over a Sn atom.

$2\sqrt{3}R30^\circ$ cell ($3 \times 3 \times 1$ k-point grid; coverage, 1/12 monolayer). Increased Pt–Sn nearest-neighbor distances (2.86 Å) due to the larger covalent radius of Sn as well as the outward relaxation of the Sn atoms, amounting to 0.27 Å on $\text{Pt}_2\text{Sn}(111)$ and 0.31 Å on $\text{Pt}_3\text{Sn}(111)$, are correctly reproduced compared to LEED (low-energy electron diffraction) results.

During geometry optimization the degrees of freedom of the two uppermost metal layers and of the adsorbed molecule have been fully relaxed, whereas during the numerical vibrational analysis, only the molecular degrees of freedom have been considered, hence neglecting any coupling between molecular modes and surface phonons. HREELS loss intensities are derived from the dynamical dipole moments along the surface normal multiplied by an instrument specific function and the inverse of the loss frequency.^{14,20,31}

3. Results and Discussion

3.1. Adsorption on Pt(111). Crotonaldehyde exists in the four energetically close E and Z isomers of the (s)-trans and (s)-cis rotamers. The analysis of the HREEL spectra of crotonaldehyde using the vibrational frequencies and intensities from DFT leads to the identification of five structures matching the experimental data. These structures, i.e., the η^2 -di σ (CC)-E-(s)-trans, η^2 -di σ (CC)-E-(s)-cis, η^3 -di σ (CC)- σ (O)-E-(s)-cis, η^4 -di σ (CC)-di σ (CO)-E-(s)-trans, and η^4 - π (CC)-di σ (CO)-E-(s)-cis complexes, have very similar stabilities (−69 to −80 kJ/mol (for schemes of the η^1 - η^4 adsorption configurations, see Figure 1 and refs 20 and 36)).

The adsorption of (s)-trans and (s)-cis prenal on Pt(111) is very similar. In combination with DFT, the HREEL spectra recorded after annealing the sample to 205 K are interpreted as a mixed phase of adsorption structures that are of the same types

of coordination as found for crotonaldehyde: η^2 -di σ (CC)-(s)-trans, η^2 -di σ (CC)-(s)-cis, η^3 -di σ (CC)- σ (O)-(s)-cis, η^4 -di σ (CC)-di σ (CO)-(s)-trans, and the η^4 - π (CC)-di σ (CO)-(s)-cis. The most stable adsorption structures for prenal computed at a low coverage of 1/9 monolayer show adsorption energies (−47 to −59 kJ/mol), which are 20–30% weaker than the corresponding crotonaldehyde forms.

No significant coverage dependence of the vibrational fingerprints has been found by comparison of calculations of prenal in the (3×3) unit cell to smaller (2×2) and (3×2) units cells, consistent with the absence of detectable vibrational shifts in experimental HREEL spectra for varying sub-monolayer doses. Nonetheless, the coverage increase leads to sizable destabilization of several structures, particularly of the η^3 and η^4 forms. The adsorption energies of η^2 -di σ (CC) structures of (s)-trans and (s)-cis decreased from −54 and −48 kJ/mol at 1/9 monolayer to −46 and −41 kJ/mol at 1/6 monolayer coverage. For the η^3 -(s)-cis and η^4 -(s)-cis structures we obtained more sizable weakenings from −50 to −38 kJ/mol and from −47 to −37 kJ/mol, respectively. Even more pronounced is the decrease for the η^4 -(s)-trans form, being almost 50% from −59 to −31 kJ/mol.

To rationalize the decrease in the adsorption energies of corresponding coordination types from crotonaldehyde to prenal, the interaction strength of the molecules to the surface and also the additional Pauli repulsion between the molecule and the surface⁴⁴ created by the new methyl substituent on the β -carbon have to be considered. An intuitive approximation to analyze the true interaction strength is the decomposition of the adsorption energy into three constituents:⁴⁵ the deformation energy costs for relaxing the surface and the molecule upon forming the adsorbate complex from their respective isolated

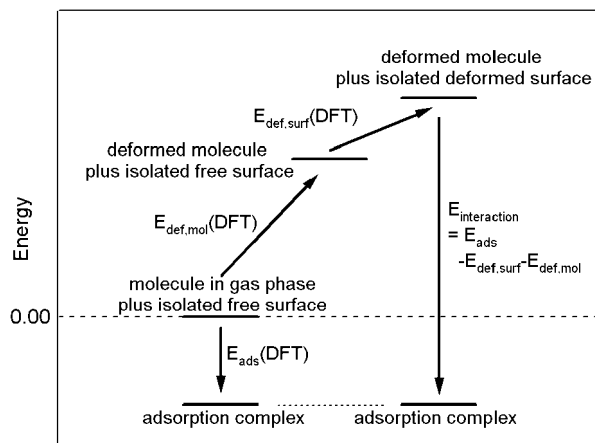


Figure 2. Decomposition of the adsorption energies into the constituting deformation energies required to distort the adsorbate and the surface in order to form the geometry for optimal bonding, and the resulting interaction energies between them.

structures, both of which are positive, and the gain of interaction energy between the already deformed fragments (Figure 2):

$$E_{\text{ads}} = E_{\text{def,surf}} + E_{\text{def,mol}} + E_{\text{int}} \quad (1)$$

The surface $E_{\text{def,surf}}$ and the molecule $E_{\text{def,mol}}$ deformation energies can be obtained by computation of the total energy of each partner isolated with a geometry frozen to the structure that it adopts in the final adsorption complex. The interaction energies E_{int} can be calculated as the binding energies between the frozen deformed fragments (molecule and surface) or from eq 1 as the difference between adsorption energy and deformation energies. However, this simple energy decomposition scheme is only strictly applicable as long as the electron transfer between the molecule and the surface remains small, which is expected in the present case of chemisorption on a metal surface.

In general the energy cost invested on Pt(111) into perturbing the surface metal atoms into a geometry optimal for interaction with the molecules is relatively small, while the distortion of the molecule is much costlier (Table 1). Especially notable is the small difference in E_{int} between crotonaldehyde and prenol. $E_{\text{def,mol}}$ and $E_{\text{def,surf}}$ vary more, which is the principal reason for the decrease of E_{ads} in the case of prenol.

For the vertical, low-hapticity η^1 types only relatively small interaction energies are found on Pt(111) because the relaxations of surface and molecule are almost negligible. This is consistent with the similarity of the optimized geometries to the gas-phase structures.^{20,36} Also the surfaces are only weakly perturbed by an outward relaxation of the bonding Pt atoms (~ 0.05 Å) and minor rearrangements of surrounding atoms.

In contrast, the η^2 and the high-hapticity η^3 and η^4 configurations of both aldehydes show considerable surface relaxations and, hence, the surface deformation costs are slightly higher (~ 20 kJ/mol). Due to Pauli repulsion and steric demand of the additional second methyl substituent, which results in further relaxations of the Pt atoms, these are on average larger for prenol (by ~ 5 kJ/mol).

The molecule distortion energies are the largest components for the flat coordination types and vary significantly with changing hapticity and bonding mechanism. They are bigger for structures interacting via a $\text{di}\sigma(\text{CC})$ mechanism than for those exhibiting $\pi(\text{CC})$ bonding, as evidenced by the comparison of the $\eta^2\text{-}\pi(\text{CC})$ and $\eta^2\text{-di}\sigma(\text{CC})$ forms. For the η^2 and η^3 structures

the distortion requires roughly ~ 150 kJ/mol, veindicating that the $\text{di}\sigma(\text{CC})$ bonding is almost solely responsible for the relaxation process. The $\eta^4\text{-di}\sigma(\text{CC})\text{-di}\sigma(\text{CO})$ structures formed by (s)-trans isomers on Pt result in higher values of ca. $\sim 211\text{--}238$ kJ/mol since their interaction takes place through both double bonds. The $\eta^4\text{-di}\sigma(\text{CC})\text{-}\pi(\text{CO})$ adsorbates of the (s)-cis isomers, in contrast, are less distorted from the gas-phase geometries (~ 110 kJ/mol) due to the weaker $\pi(\text{CO})$ coordination.

The effect of the substitution on the β -carbon is also evident in the molecule deformation costs: On average we compute ~ 16 kJ/mol higher deformation energies for prenol (ca. 164 kJ/mol vs 148 kJ/mol for crotonaldehyde for strongly bonded $\eta^2\text{-}\eta^4$ forms), which are caused by the need to relieve the larger Pauli repulsions of the molecule with the surface compared to crotonaldehyde. This is evidenced nicely by the larger outward relaxations of bonding metal atoms below the C=C moiety (0.02–0.09 Å) in the case of prenol. Indeed the outward relaxation of the metal atoms directly bonded to the carbons is a way to increase the separation between the molecule and the surface and, hence, to reduce the Pauli repulsion.

The structural variations between the corresponding adsorption geometries of both molecules are minor for most of the bond lengths such as particularly the C1=O , C1-C2 , and C2=C3 bonds and the hydrogen bond distances (deviations < ca. ± 0.01 Å). This suggests that the internal bond strengths are almost unaffected by the substitution.

The molecule–surface bonds of the aldehydic part agree closely in the various adsorption geometries (variations of the bond lengths: $\Delta r(\text{O-Pt})$ and $\Delta r(\text{C1-Pt}) < \pm 0.01$ Å; absolute values of $r(\text{O-Pt}) \approx 2.25$ and $r(\text{C1-Pt}) \approx 2.15$ Å for σ bonds, respectively), and also $r(\text{C2-Pt})$ is very similar ($< \pm 0.01$ Å; ca. 2.14–2.20 Å). The C3-Pt bond from the vinylic moiety of prenol in contrast shows slightly larger elongations in comparison to crotonaldehyde (by 0.02–0.04 Å; ca. 2.14–2.18 Å). Quite similarly for the configurations interacting by a $\pi(\text{CC})$ mechanism, such as for example the $\eta^4\text{-}\pi(\text{CC})\text{-di}\sigma(\text{CO})$ forms, the additional methyl substituent leads to a stronger tilting of the C2=C3 axis (for prenol around 9°) away from the surface plane (for crotonaldehyde, 1.5°). Here the second methyl group leads to a stretching of $r(\text{C3-Pt})$ by 0.07–0.09 Å to typically ~ 2.30 Å for prenol.

Importantly, the relaxation of the interacting Pt atoms out of the substrate is found to be generally about 10% larger for prenol (by 0.02–0.05 Å) than for crotonaldehyde, consistent with the slightly larger surface deformation energies. The displacements of the relaxed Pt atoms parallel to the surface plane induced by the bonding are of similar size (on average < 0.05 Å). Only for the η^4 complexes a few slightly larger displacements of up to 0.1 Å are noticed. Typically the surface atoms bonded to carbon atoms are displaced outward by 0.07–0.25 Å for prenol, whereas the protrusions induced by crotonaldehyde on the Pt(111) surface were around 0.08–0.20 Å. In contrast, the relaxation effects are much less pronounced for the Pt atoms bonding to the aldehydic oxygens (between 0.05 and 0.08 Å).

The interaction energies computed finally according to eq 1 are very similar for both molecules in corresponding coordination types and do not show a simple dependence on the hapticity (Table 1). The $\eta^2\text{-di}\sigma(\text{CC})$ forms are interacting as strongly as the $\eta^3\text{-di}\sigma(\text{CC})$ forms, but weaker than the $\eta^4\text{-di}\sigma(\text{CC})$ bonding. Therefore the decrease of the adsorption energies of ca. 20–25 kJ/mol from crotonaldehyde to prenol arises primarily from larger distortion energies due to increased Pauli repulsions. This,

TABLE 1: Decomposition of the Adsorption Energies of Crotonaldehyde and Preenal on Pt(111) ($\Theta = 1/9$ monolayer) in the Constituting Surface and Molecule Deformation Costs and the Interaction Energy (All Energies in kilojoules per mole)

Pt(111), $\Theta = 1/9$ monolayer	$E_{\text{def, surf}}$	$E_{\text{def, mol}}$	E_{int}	E_{ads}
crotonaldehyde:				
η^1 -top-E-(s)-trans	10	7	-40	-24
η^2 - π (CC)-E-(s)-trans	26	47	-118	-44
η^2 -di σ (CC)-E-(s)-trans	17	144	-237	-76
η^2 -di σ (CC)-E-(s)-cis	16	141	-230	-74
η^3 -di σ (CC)- σ (O)-E-(s)-cis	18	136	-231	-77
η^4 -di σ (CC)-di σ (CO)-E-(s)-trans	17	211	-307	-80
η^4 -di σ (CC)- π (CO)-E-(s)-cis	23	106	-198	-69
preenal:				
η^1 -top-(s)-trans	10	5	-47	-32
η^2 - π (CC)-(s)-trans	31	50	-113	-32
η^2 -di σ (CC)-(s)-trans	22	158	-234	-54
η^2 -di σ (CC)-(s)-cis	21	148	-216	-48
η^3 -di σ (CC)- σ (O)-(s)-cis	23	162	-235	-50
η^4 -di σ (CC)-di σ (CO)-(s)-trans	19	238	-316	-59
η^4 -di σ (CC)- π (CO)-(s)-cis	30	115	-192	-47

however, is not accompanied by a change in the interaction energies as we will show in the following using the vibrational frequencies.

Taking into account shifts due to the different substitution of the β -carbon, the vibrational properties of the crotonaldehyde vs preenal structures support the energetic analysis above. However, changes of the normal coordinate basis from crotonaldehyde to preenal lead to frequency changes that do not directly reflect changes in the adsorption energy, which renders this analysis more difficult. Despite these complications, we can conclude clearly that the vibrational frequencies and their shifts of corresponding configurations do not reflect with the strongly varying adsorption energies E_{ads} but are more in line with the similarity of the interaction energies E_{int} .

The case of the vertical η^1 -top-(s)-trans configurations obtained from DFT can serve as a simple example that underlines the correlation of frequencies and interaction energy: The $\nu(\text{Pt}-\text{O})$ stretching modes are obtained at 107 and 125 cm^{-1} for crotonaldehyde and preenal, respectively. This exemplifies the close, though slightly weaker, interaction of crotonaldehyde with the surface (-40 and -47 kJ/mol, respectively). Consistently, the indirectly perturbed $\nu(\text{C}=\text{O})$ normal modes of these structures are shifted by $\sim 140 \text{ cm}^{-1}$ to 1562 cm^{-1} (gas phase, 1706 cm^{-1}) and 1545 cm^{-1} (gas, 1679 cm^{-1}) for the E-(s)-trans crotonaldehyde and (s)-trans preenal structures. Clearly, the similarity of shifts and $\nu(\text{Pt}-\text{O})$ frequencies cannot be explained satisfactorily by the adsorption energies that differ by $\sim 30\%$ (crotonaldehyde, -24 kJ/mol; preenal -32 kJ/mol).

For the flat adsorption forms of both molecules, the analysis is complicated significantly by strong changes in the normal coordinate basis of the vibrations that are traced back to the stronger deformation of preenal caused by the additional methyl substituent. If these normal basis changes are neglected, the comparison of vibrations can lead to wrong conclusions about the interaction to the surface, as can be illustrated for the η^2 -di σ (CC) forms of E-(s)-trans crotonaldehyde and (s)-trans preenal (Table 2). The antisymmetric molecule-surface vibrations $\nu_{\text{as}}(\text{PtC}2-\text{PtC}3)$ are computed for crotonaldehyde and preenal at 519 and 591 cm^{-1} , and the corresponding symmetric $\nu_s(\text{PtC}2-\text{PtC}3)$ modes are found at 348 and 511 cm^{-1} , respectively. This suggests a substantially stronger surface bonding of preenal—in apparent contradiction to the computed adsorption energies, which are 30% weaker for preenal (-54 kJ/mol vs -76 kJ/mol for crotonaldehyde). In this case, the different couplings with other vibrations lead to shifts because

the eigenfrequencies of the normal modes do not purely depend on the stretching vibrations.

Among the internal modes, which are indirectly affected by the adsorption, the $\nu(\text{C}2=\text{C}3)$ modes show larger disagreements, whereas the shifts for the $\nu(\text{C}1=\text{O})$ modes, for instance, are in much better agreement for corresponding configurations of both molecules. Thus, for example the $\nu(\text{C}2=\text{C}3)$ modes of the η^3 structures of crotonaldehyde and preenal are shifted by 510 and 426 cm^{-1} due to adsorption, whereas the $\nu(\text{C}1=\text{O})$ are more consistently shifted by 270 and 246 cm^{-1} . Similar observations can be made for the remaining η^2 and η^4 structures.

Taking the coupling changes and substitution effect into account, we therefore conclude that the vibrational properties of corresponding configurations are in better agreement with the relatively small changes of the *interaction energies* than with the significantly changes of the *adsorption energies*. The substantial weakening in the adsorption energies of preenal as compared to crotonaldehyde by ca. 30% is not reflected in the vibrational shifts. Thus, to summarize the adsorption on Pt(111), we find that interaction energy E_{int} is a much better parameter than the adsorption energy E_{ads} to understand the vibrational properties of multifunctional molecules interacting with surfaces. Clearly the trends of the adsorption energies due to coordination and substitution effects do not follow changes in the interaction energy hand in hand but require one to take the deformation energies into account. The adsorption energy is a complex balance of energetic contributions due to adsorbate complex formation, while the vibrational frequencies reflect the properties of the final adsorption state.

3.2. Adsorption on the Pt₃Sn(111) and Pt₂Sn(111) Surface Alloys

A crucial question that needs to be answered for a deeper understanding of the selective hydrogenation of the α,β -unsaturated aldehydes is how alloying changes their initial interaction with the catalyst.

The adsorption configurations of crotonaldehyde identified on the Pt₃Sn(111) surface alloy are surprisingly similar to those on Pt(111) despite the presence of the Sn atoms. From the analysis of the HREELS spectra by the aid of the DFT calculations, several structures have been revealed: at high coverages, the η^2 -di σ (CC)-E-(s)-trans and η^2 -di σ (CC)-E-(s)-cis structures and two energetically competitive η^1 -top-E-(s)-trans-OSn form on both surface alloys; at low coverages the η^2 -di σ (CC)-E-(s)-trans, the η^3 -di σ (CC)- σ (O)-E-(s)-cis-OSn, and the η^4 - π (CC)-di σ (CO)-E-(s)-cis-OSn forms coexist. On Pt₃Sn, also the η^2 -di σ (CC)-E-(s)-cis structure, which is not stable on

TABLE 2: Important Vibrational Normal Modes (cm^{-1}) of Selected Structures of Crotonaldehyde and Prenal on Pt(111) ($\Theta = 1/9$ monolayer)^a

Pt(111), $\Theta = 1/9$ monolayer	$\nu(\text{C1=O})$	$\nu(\text{C1-C2})$	$\nu(\text{C2=C3})$	$\nu_s(\text{PtO-PtC1})$ or $\nu(\text{Pt-O})$	$\nu_{\text{as}}(\text{PtO-PtC1})$	$\nu_s(\text{PtC2-PtC3})$	$\nu_{\text{as}}(\text{PtC2-PtC3})$
crotonaldehyde:							
η^1 -top-E-(s)-trans	1562	1154	1633	107			
η^2 - π (CC)-E-(s)-trans	1671	1040	1446		309	399	
η^2 -di σ (CC)-E-(s)-trans	1686	1024	1115		348	519	
η^2 -di σ (CC)-E-(s)-cis	1610	993	1109		441	554	
η^3 -di σ (CC)- σ (O)-E-(s)-cis	1443	1025	1111	302	351	539	
η^4 -di σ (CC)-di σ (CO)-E-(s)-trans	1172	988	1100	289	369	452	542
η^4 -di σ (CC)- π (CO)-E-(s)-cis	1159	974	1205	283	325	402	520
E-(s)-trans gas phase	1706	1143	1642				
E-(s)-cis gas phase	1713	1008	1621				
prenal:							
η^1 -top-(s)-trans	1545	1154	1618	125			
η^2 - π (CC)-(s)-trans	1660	1070	1379		379	460	
η^2 -di σ (CC)-(s)-trans	1666	1039	1189		511	591	
η^2 -di σ (CC)-(s)-cis	1655	1036	1205		415	559	
η^3 -di σ (CC)- σ (O)-(s)-cis	1453	1063	1181	367	690/361*	539	
η^4 -di σ (CC)-di σ (CO)-(s)-trans	1164	1020	1184	281	417	480	554
η^4 -di σ (CC)- π (CO)-(s)-cis	1186	935	1389*	280	343	437	512
(s)-trans gas phase	1679	1130	1637				
(s)-cis gas phase	1699	1089	1607				

^a The values for the corresponding gas-phase isomers of both aldehydes are given for comparison. Note that values marked with an asterisk (*) show large changes in the vibrational couplings as compared to the corresponding modes of crotonaldehyde, which have been omitted for sake of clarity. Particularly a stronger coupling of molecule–metal and C–C stretching vibrations to γ and δ modes of the carbon backbone occur. In case of the η^4 modes, all four molecule-surface stretching vibrations are strongly coupled to each other.

Pt_2Sn , agrees with the experiments. Notably, all obtained structures involving a coordination of the aldehydic function require an oxygen–tin bond in order to be sizably stable.

Prenal, unlike crotonaldehyde, shows significant differences in the adsorption behavior on both Pt–Sn model catalysts. We identified two η^1 -top-(s)-trans-OSn geometries on $\text{Pt}_3\text{Sn}(111)$, and also on the $\text{Pt}_2\text{Sn}(111)$ only η^1 -top-(s)-trans-OSn adsorption structures are found for prenal, yet here they are strongly tilted toward the surface.

The TPD/TPRS experiments^{20,36} on the Pt–Sn surface alloys show that the bonding with the surface is considerably weakened since only low-temperature desorption states are measured and the decomposition at higher temperatures is suppressed. This is consistent with the reduced adsorption energies obtained for the identified structures from DFT^{20,36} (Table 3). This decrease from Pt(111) to $\text{Pt}_3\text{Sn}(111)$ and $\text{Pt}_2\text{Sn}(111)$ implies a significant weakening of the bonding to the surface, which was previously suggested to be caused by an increase in the electron transfer from Sn to Pt and a d-band center lowering²⁶ in accordance with the d-band model.⁴⁶ Indeed, since similar structures of all coordination types (η^2 , η^3 , and η^4) are obtained on all model catalyst surfaces as local minima in DFT, the weakening of the adsorption energy initially appears to be governed primarily by electronic effects. No true *ensemble effect* in the sense of Sachtler,⁴⁷ i.e., a site-blocking that eliminates certain configurations, is observed, although structures with higher hapticities, in particular η^4 forms, are destabilized preferentially and most η^1 , η^3 , and η^4 configurations change from O–Pt to O–Sn bonding.

A closer look at the geometries and the vibrational frequencies of the adsorption structures reveals, however, surprising inconsistencies with the simple argumentation based on electronic effects. Generally, the geometries are very similar for a given coordination on the three surfaces, which holds true in particular for the C2=C3 and C1=O bond lengths and the surface bonds that should be affected significantly by changing the adsorption energies (see refs 20 and 36 for structure details). Moreover,

the vibrational properties of the corresponding structures are also surprisingly similar, contrary to what might be inferred from the strongly decreasing adsorption energies.

An instructive example for these “inconsistencies” is given by the η^1 -top structures. In case of prenal, the most stable η^1 forms of the (s)-trans isomer show an increase of the adsorption energy from -32 kJ/mol on Pt(111) to -39 and -33 kJ/mol on Pt_3Sn and $\text{Pt}_2\text{Sn}(111)$, respectively, which goes along with a change of coordination from Pt to Sn atoms. This increase in adsorption energy is unique to the η^1 forms and caused by the character of the interactions, being partially through an oxygen lone pair and partially electrostatic. Here the bonding is strengthened by interaction with the electron deficient Sn. In contrast, the interaction of the flat forms with di σ (C=O) or $\pi(C=O)$ coordination occurs mainly through the $\pi(\text{CO})$ and $\pi^*(\text{CO})$ orbitals, but since the latter cannot receive electrons from the deficient Sn, these bonding mechanisms are disfavored on the alloys.

However, despite the increase in adsorption energies, the vibrational properties point to a weaker interaction energy: Both the $\nu(\text{M}-\text{O})$ metal–molecule stretching modes, which are the primary indicators of the adsorption strength, and the indirectly perturbed internal vibrations, foremost $\nu(\text{C1=O})$ and $\nu(\text{C2=C3})$, point to a decrease of the force constants (Table 4 and Figure 3). Since the metal atoms were frozen, i.e., both Sn and Pt were essentially treated with infinite mass, and the coupling to metal phonons has been ignored, the analysis of the $\nu(\text{M}-\text{O})$ frequencies in a harmonic picture is valid. Indeed, the reduced masses for both vibrations are very similar (4% deviation), and hence the frequency changes can be interpreted largely as changes in the force constants.

The $\nu(\text{M}-\text{O})$ frequencies of the η^1 prenal decrease from 125 cm^{-1} on Pt(111) to ~ 104 – 109 cm^{-1} on the surface alloys, and similarly the $\nu(\text{C1=O})$ modes shift from 1545 cm^{-1} to a far less perturbed value around $\sim 1588 \text{ cm}^{-1}$. Hence, contrasting the behavior of the adsorption energies the bonding must in fact be slightly weaker than on Pt(111).

TABLE 3: Analysis of the Adsorption Energies of Crotonaldehyde and Prenal on Pt–Sn/Pt(111) Surface Alloys (All Energies in kilojoules per mole)

molecule/surface	$E_{\text{def,surf}}$	$E_{\text{def,mol}}$	E_{int}	E_{ads}
crotonaldehyde/Pt ₃ Sn(111)				
η^1 -top-E-(s)-trans-OSn	2	2	-37	-33
η^2 -di σ (CC)-E-(s)-trans	41	149	-222	-33
η^2 -di σ (CC)-E-(s)-cis	40	154	-228	-34
η^2 -di σ (CC)- σ (O)-E-(s)-cis-OSn	35	144	-230	-51
η^4 -di σ (CC)-di σ (CO)-E-(s)-trans-OSn	34	206	-278	-38
η^4 -di σ (CC)- π (CO)-E-(s)-cis-OSn	37	110	-189	-42
crotonaldehyde/Pt ₂ Sn(111), $\Theta = 1/6$				
η^2 -di σ (CC)-E-(s)-trans	62	158	-240	-20
η^2 -di σ (CC)-E-(s)-cis	66	164	-260	-30
η^4 -di σ (CC)- π (CO)-E-(s)-cis-OSn	44	108	-168	-16
crotonaldehyde/Pt ₂ Sn(111), $\Theta = 1/9$				
η^1 -top-flat-E-(s)-trans-OSn	3	0	-31	-28
η^2 -di σ (CC)-E-(s)-trans	56	146	-235	-34
η^3 -di σ (CC)- σ (O)-E-(s)-cis-OSn	47	139	-235	-49
η^4 -di σ (CC)- π (CO)-E-(s)-cis-OSn	49	113	-191	-29
prenal/Pt ₃ Sn(111)				
η^1 -top-(s)-trans-OSn	2	2	-43	-39
η^1 -top-(s)-trans-OSn(2)	3	2	-36	-31
η^2 - π (CC)-(s)-trans	59	52	-112	-1
η^2 -di σ (CC)-(s)-trans	47	167	-224	-10
η^3 -di σ (CC)- σ (O)-(s)-cis-OSn	44	168	-232	-20
η^4 -di σ (CC)-di σ (CO)-(s)-trans-OSn	46	244	-306	-17
η^4 -di σ (CC)- π (CO)-(s)-cis-OSn	60	146	-217	-11
prenal/Pt ₂ Sn(111)				
η^1 -top-(s)-trans-OSn	4	0	-37	-33
η^2 - π (CC)-(s)-trans	74	40	-120	-5
η^2 -di σ (CC)-(s)-trans	68	150	-225	-6
η^3 -di σ (CC)- σ (O)-(s)-cis-OSn	59	156	-232	-7
η^4 -di σ (CC)- π (CO)-(s)-cis-OSn	55	107	-166	-17

TABLE 4: Important Vibrational Normal Modes Selected Structures of Crotonaldehyde and Prenal on Pt₃Sn(111) ($\Theta = 1/12$ monolayer) and on Pt₂Sn(111) ($\Theta = 1/9$ monolayer) (All Values in cm⁻¹)^a

molecule/surface	$\nu(\text{C1=O})$	$\nu(\text{C1-C2})$	$\nu(\text{C2=C3})$	$\nu_s(\text{PtO-PtC1})$ or $\nu(\text{Pt-O})$	$\nu_{\text{as}}(\text{PtO-PtC1})$	$\nu_s(\text{PtC2-PtC3})$	$\nu_{\text{as}}(\text{PtC2-PtC3})$
crotonaldehyde/Pt ₃ Sn(111)							
η^1 -top-E-(s)-trans-OSn	1611	1157	1635	127			
η^2 -di σ (CC)-E-(s)-trans	1674	1039	1124		345	524	
η^2 -di σ (CC)-E-(s)-cis	1641	1003	1128		452	548	
η^3 -di σ (CC)- σ (O)-E-(s)-cis-OSn	1460	1036	1124	316	335	533	
η^4 - π (CC)-di σ (CO)-E-(s)-cis-OSn	1166	978	1454	234	302	397	515
crotonaldehyde/Pt ₂ Sn(111), $\Theta = 1/6$							
η^2 -di σ (CC)-E-(s)-trans	1663	1037	1088		326	531	
η^2 -di σ (CC)-E-(s)-cis	1636	984	1125		468/320*	564	
η^4 - π (CC)-di σ (CO)-E-(s)-cis-OSn	1156	982	1460	246	313	396	511
crotonaldehyde/Pt ₂ Sn(111), $\Theta = 1/9$							
η^1 -top-(s)-trans-OSn	1612	1177	1631	103			
η^2 -di σ (CC)-E-(s)-trans	1661	1037	1081		328	525	
η^3 -di σ (CC)- σ (O)-(s)-cis-OSn	1451	1035	1125	313	322	526	
η^4 - π (CC)-di σ (CO)-(s)-cis-OSn	1158	981	1459	245	310	401	519
prenal/Pt ₃ Sn(111)							
η^1 -top-(s)-trans-OSn	1584	1156	1615	104			
η^1 -top-(s)-trans-OSn(2)	1588	1154	1616	108			
η^2 - π (CC)-(s)-trans	1648	1076	1389		329	461	
η^2 -di σ (CC)-(s)-trans	1662	1048	1192		346	579	
η^3 -di σ (CC)- σ (O)-(s)-cis-OSn	1488	1068	1187	270	356	538	
η^4 -di σ (CC)-di σ (CO)-(s)-trans-OSn	1172	1029	1190	252	442	482	547
η^4 - π (CC)-di σ (CO)-(s)-cis-OSn	1217	915	1441	234	336	397	543
prenal/Pt ₂ Sn(111)							
η^1 -top-(s)-trans-OSn	1592	1149	1616	110			
η^2 - π (CC)-(s)-trans	1664	1092	1397		335	464	
η^2 -di σ (CC)-(s)-trans	1640	1061	1198		410/323*	565	
η^3 -di σ (CC)- σ (O)-(s)-cis-OSn	1480	1076	1190	301	350	543	
η^4 - π (CC)-di σ (CO)-(s)-cis-OSn	1194	930	1456	215	332	425	512

^a Note that for the molecule–metal stretching vibrations any couplings to other vibrations, in particular the δ modes of the carbon backbone, have been omitted (*). In the case of the η^4 modes, all four molecule–surface stretching vibrations are usually strongly coupled.

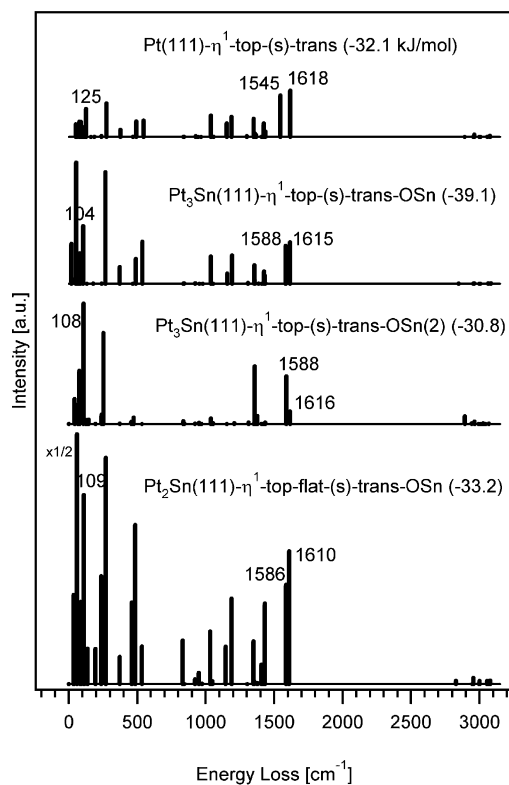


Figure 3. Comparison of the computed HREEL spectra (dipole scattering limit, 4.7 eV, 60° specular) of the η^1 configurations of (s)-trans prenalen on the three model catalysts. Note that the structures on the surface alloy are coordinated to Sn atoms. Clearly strong changes of the relative loss intensities can be observed, whereas the alloying does not lead to significant frequency shifts.

The solution to the inconsistencies between increasing adsorption energies and the opposite behavior of the vibrational properties comes again from the analysis of the energy contributions to the adsorption energy (Table 3). The crucial differences are the surface deformation energies on the Pt–Sn surfaces: while the energetic cost to shape the adsorption site are almost negligible on the surface alloys, the lifting of a bonding metal atom on Pt(111) required ca. 10 kJ/mol. Similar to Pt(111) (Table 1), the molecule distortion energies remain negligible for all η^1 forms on the surface alloys, which in combination with the adsorption energies then leads to a decrease of the interaction strength by alloying: the strongest interaction is calculated on Pt(111) (-47 kJ/mol), whereas it is generally weaker on the Pt–Sn surface alloys (~ -40 kJ/mol on average on Pt₃Sn(111) and -37 kJ/mol on Pt₂Sn(111)). Thus, alloying weakens the interaction strength, and, hence, the peculiar behavior of vibrational frequencies of the η^1 structures can be understood.

Evidently the adsorption energy is also in this case not a good measure of the true interaction between the molecule and the surface. It actually masks a very different energy compromise: on Pt(111), interaction energies are large but the surface deformations have a significant cost, whereas, on Pt–Sn, the interaction energy is decreased by $\sim 15\%$ (with implications on the vibrational frequencies) and the deformation cost is almost completely negligible.

Surprisingly, despite the decrease in surface deformation energies of the η^1 forms on the Pt–Sn surfaces, the absolute relaxations of the metal atoms are found to be even slightly larger than on Pt(111): around ~ 0.15 Å on Pt₃Sn and even 0.25 Å on Pt₂Sn vs only ~ 0.09 Å for the η^1 structures on the pure Pt surface.

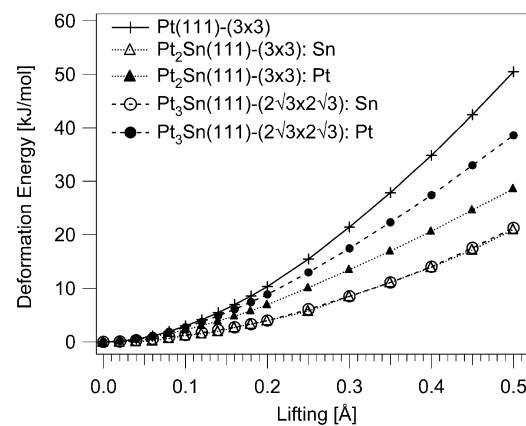


Figure 4. Energy costs (kJ/mol) for the lifting of metal atoms on the three model catalysts. In a simple approach, the atoms have been lifted up from their respective equilibrium positions without further relaxation of the surrounding.

To understand the changes in surface relaxation, we modeled the outward lifting of the Pt and Sn atoms on the three surfaces, which has been reported partially already in ref 48. The surrounding substrate (Figure 4) atoms have been frozen in this approximation. For the range of relaxations between 0.05 and 0.2 Å usually found in the adsorbate structures, the energetic costs for a single atom are comparably small (<10 kJ/mol) on all surfaces. The cost of lifting up Pt further is higher than that of Sn, which can be moved up with similar energy requirements on both surface alloys. For the Pt atoms, the outward relaxation becomes “cheaper” with increasing amount of Sn, indicating that its bonds in the metal matrices are weakened and that surface stress due to the incorporation of the larger Sn atoms is being relaxed.

Approximating the surface deformation energies for the η^1 structures from the approximated potential energy curves suggests that the deformation costs should be slightly smaller on the two Pt–Sn surfaces, which we also find in the detailed energy analysis. However, lifting up a single Sn atom by the value found in the adsorption complex leads to a slight overestimation of the surface deformation cost since the relaxation of the metal atoms in the environment is ignored in the crude model. A major difference in the surface relaxations induced by adsorption on Pt₂Sn versus the other model catalysts is the occurrence of significant in-plane rearrangements in the first metal layer, which effectively reduce the surface strain and deformation terms. The metal atoms in the immediate surroundings of the Sn atom lifted by the η^1 structures are displaced by up to ~ 0.15 Å on the tin-richest surface alloy, whereas on Pt(111) and Pt₃Sn(111) displacements of ~ 0.02 and ~ 0.05 Å are computed on average.

Our findings for the flat η^2 , η^3 , and η^4 structures are very similar and shall be exemplified by the η^2 -di σ (CC) and η^3 -di σ (CC)- σ (O) forms of crotonaldehyde in more detail. The conclusions drawn are generally valid for all flat structures of crotonaldehyde and prenalen on the three investigated surfaces.

The comparison of the HREEL spectra (Figure 5) for the η^2 -di σ (CC) configurations of E-(s)-trans crotonaldehyde on the different surfaces reveals close similarities despite the weakening of the adsorption energies from -76 kJ/mol on Pt(111) to -33 and -34 kJ/mol on Pt₃Sn(111) and Pt₂Sn(111) ($\Theta = 1/9$ monolayer), respectively. Also the structural parameters are very close on the three substrates. Likewise also the η^3 -di σ (CC)- σ (O)-E-(s)-cis structures suffer a sizable weakening of their adsorption energies from -77 kJ/mol on pure Pt to -51 and

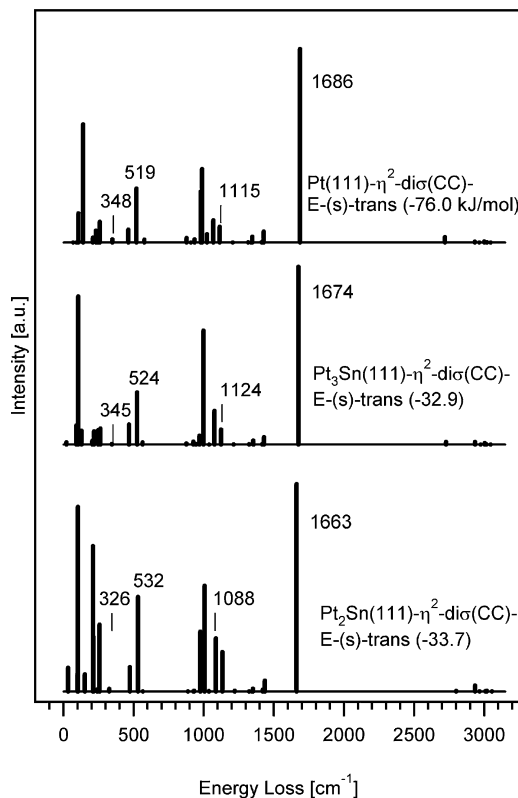


Figure 5. Computed HREEL spectra (dipole scattering limit, 4.7 eV, 60° specular) of the η^2 configurations of E-(s)-trans crotonaldehyde on Pt(111) and the Pt_xSn(111) surfaces ($x = 2, 3$). The bonding of these structures is always to two neighboring Pt atoms. Despite the alloying and the decrease of the adsorption energies, the vibrational properties remain very similar on all model catalysts.

–49 kJ/mol on Pt₃Sn(111) and Pt₂Sn(111), but again the similar vibrational spectra (Figure 6) and optimized geometries suggest a rather similar interaction with the surfaces. The behavior of the structural parameters and vibrational properties of both examples are at variance with the strong decrease in adsorption energies, which has hitherto been explained by the d-band lowering from Pt(111) to Pt₃Sn and to Pt₂Sn²⁶ (from –1.93 eV to –2.09 and –2.12 eV, respectively²⁶). The lowering of the d-band center is much less pronounced, particularly between both surface alloys, and, thus, agrees much better with the trend in the interaction energies.

The molecule deformation energies of the crotonaldehyde η^2 -diσ(CC) and η^3 -diσ(CC)-σ(O) forms (Table 3) of on average ca. 150 kJ/mol on the surface alloys show only small increases by the alloying, consistent with the close agreement of the geometries to those on Pt(111). They remain slightly smaller for crotonaldehyde as compared to the corresponding structures of prenal (ca. 160 kJ/mol) due to the increased steric effects of the second methyl group of the latter. For the highest-hapticity η^4 configurations, a similar trend is observed: Here the energies invested into relaxing the molecules on the two surface alloys vary typically between ~107 kJ/mol for the η^4 -(s)-cis structures with its weaker π (CC) bonding and ~244 kJ/mol for the η^4 -diσ(CC) structure of the (s)-trans isomer; the corresponding values for crotonaldehyde are computed between ~110 and ~206 kJ/mol, respectively.

As a major effect of alloying on the adsorption, we observe significantly larger surface relaxations and, thus, higher surface deformation energies on the alloys (Table 3): The sizes of these deformations generally increase with tin content and are of the

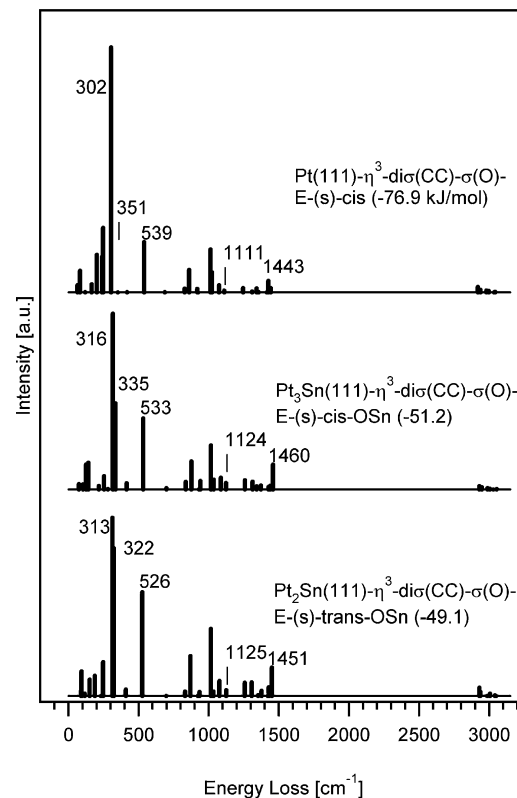


Figure 6. Computed HREEL spectra (dipole scattering limit, 4.7 eV, 60° specular) of the η^3 configurations of E-(s)-cis crotonaldehyde on Pt(111) and the Pt_xSn(111) surfaces. Again the similarities of the computed HREEL spectra are intriguing on the three model catalysts. Notice that on pure Pt the aldehydic oxygen is coordinated to Pt, whereas it bonds to Sn on the surface alloys.

same order of magnitude for corresponding flat structures of each molecule on each surface. The surface deformation energy costs increase with the Sn content from ~37 and 50 kJ/mol on average for the flat crotonaldehyde and prenal adsorption forms on Pt₃Sn to ~51 and 61 kJ/mol, respectively, on Pt₂Sn. This more than doubles the average costs for high-hapticity structures on Pt(111) (~18 and 23 kJ/mol, respectively).

For the chosen example of η^2 -diσ(CC)-E-(s)-trans crotonaldehyde, significantly increasing outward relaxations of the Pt atoms under the vinylic moiety from Pt(111) over Pt₃Sn(111) to Pt₂Sn(111) occur (Figure 7). The corresponding value increases from 0.20 via 0.31 to 0.38 Å for the atom bonding to vinylic C2, and from 0.18 via 0.32 to 0.51 Å for the one below C3.

In addition the Pt atoms below the C2=C3 bond shift by ~0.20 and 0.12 Å in the surface plane toward each other on Pt₂Sn(111), whereas the in-plane displacements are much smaller on Pt(111) and Pt₃Sn. The new Pt–Pt distance of 2.70 Å on Pt₂Sn (bulk distance of 2.82 Å) suggests that the adsorption bonding is more favorable with a slightly contracted Pt dimer. These relaxations result in the computed surface deformation energies of 41 and 56 kJ/mol for Pt₃Sn(111) and Pt₂Sn(111), respectively.

For the η^3 -diσ(CC)-σ(O)-E-(s)-cis forms, the trend is related closely: Here energy costs of 31 and 47 kJ/mol are obtained in line with increased lifting of the Pt atoms below C2 from 0.13 Å on Pt(111) to 0.26 and 0.34 Å on Pt₃Sn(111) to Pt₂Sn(111). Further, the Pt atom below C3 is relaxed outward by 0.15, 0.30, and 0.40 Å on these three surfaces, respectively. The O-metal bonding leads to much smaller outward relaxations of 0.03

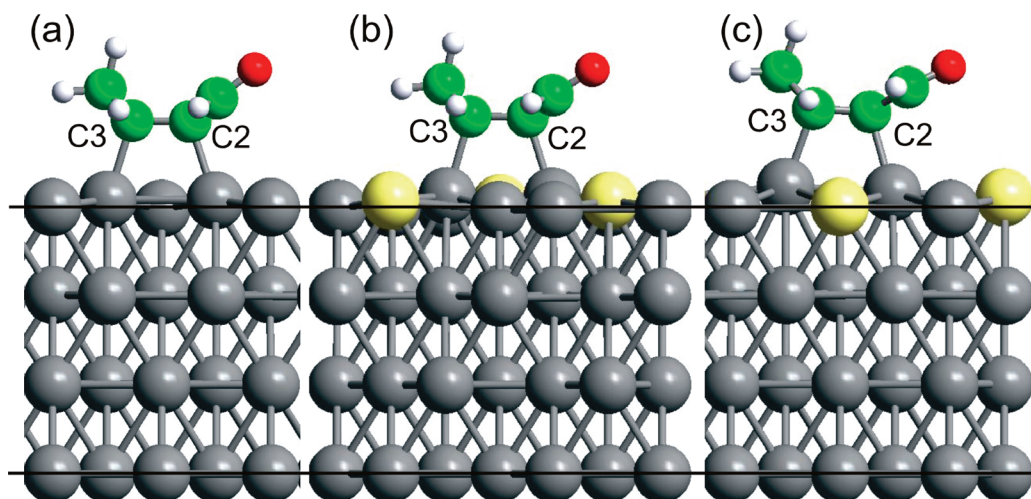


Figure 7. Illustration of the outward relaxation of the Pt atoms bonding to the vinylic moiety in the η^2 -dio(CC) configurations of E-(s)-trans crotonaldehyde on Pt(111) (a), Pt₃Sn(111) (b), and Pt₂Sn(111) (c).

(O–Pt) and 0.09 and 0.19 Å (both O–Sn) correspondingly. This suggests that this bond contributes much less to the adsorption than the dio(CC) bond. Also in this case in-plane displacements of the atoms are found on Pt₂Sn(111), namely, ca. 0.21, 0.12, and 0.13 Å below C2, C3, and O. Similar to the contraction of the Pt₂ dimer for the η^2 case, this deformation reduces the size of the “Pt₂Sn₁” 3-fold hollow site and obviously optimizes the adsorption bonding.

In general the results for the η^4 configurations follow the same trend and shall just be briefly mentioned here before turning back to our examples: The outward relaxations reach for example up to 0.45 Å for the Pt atom below the π (CC) bond of η^4 - π (CC)-dio(CO)-(s)-cis-OSn prenal and 0.36 Å for the corresponding crotonaldehyde structure. The O–Sn bond leads to lifting of the Sn atoms of 0.24 and 0.10 Å in these cases, respectively. The strong Pauli repulsion of the additional CH₃ substituent for prenal (in the Z position of the hydrogen for crotonaldehyde) causes the Sn atom beneath to be pushed inward by ~0.17 Å and sideways by ~0.11 Å, whereas for crotonaldehyde the magnitude of the relaxation is much smaller with 0.08 Å. The CH₃ group in the (s)-trans position ends up near a Sn atom and forces it to relax inward by 0.10 for prenal (0.09 Å for crotonaldehyde). Such strong inward relaxations of nearby surface atoms toward the bulk are also found for other flat configurations, particularly of prenal, but in all cases Sn atoms remain above the surface plane.

Finally we can resolve the apparent contradictions between the similarities of adsorption geometries and vibrational properties of corresponding configurations by computing the interaction energies (Table 3), which surprisingly reveal only a slight weakening of the interaction on the Pt–Sn surfaces with respect to Pt(111).

The values obtained for the crotonaldehyde η^2 -dio(CC) and η^3 -dio(CC)- σ (O) structures are quite similar: -237, -222, -235 kJ/mol on Pt(111), Pt₃Sn(111), and Pt₂Sn(111). Therefore the interaction energies correlate much better with the minor structural changes and the small vibrational shifts than the adsorption energies (Table 4). For the η^2 form, we computed the frequencies of the indirectly perturbed ν (C2=C3) stretching mode at 1115, 1124, and 1081 cm⁻¹ on Pt, Pt₃Sn, and Pt₂Sn, respectively, supporting the finding of weakly affected interaction energies. Also the ν_{as} (PtC2–PtC3) and ν_s (PtC2–PtC3) vibrations are very similar (519, 524, and 525 cm⁻¹ as well as 348, 345, and 328 cm⁻¹) and clearly rule out a significant

weakening of the bonding as implied from the strongly decreasing adsorption energies.

In the same fashion, the vibrational patterns of the η^3 examples of E-(s)-cis crotonaldehyde can be rationalized by the less affected interaction energies. A little caution must be applied here, though, since the dynamical matrices show again changes in the coupling of the normal modes. Nonetheless, our argumentation is confirmed: consistent with similar interaction energies of -231 kJ/mol on Pt(111), -230 on Pt₃Sn and -235 kJ/mol on Pt₂Sn, we find only small vibrational shifts for the ν (C2=C3) stretching modes (1111, 1124, and 1125 cm⁻¹) and weaker frequencies for the asymmetric ν_{as} (PtC2–PtC3) (539, 533, and 526 cm⁻¹) and the symmetric ν_s (PtC2–PtC3) (351, 335, and 322 cm⁻¹) vibrations. Moreover, the frequencies of the ν (O–metal) stretching mode are rather close with 302, 316, and 313 cm⁻¹ on the three surfaces although the bonding has changed from O–Pt to O–Sn.

The energetic analysis, optimized geometries, and vibrational properties of the remaining adsorption configuration of crotonaldehyde, and those of prenal, follow this trend and show much better agreement with the similar interaction energies than with decreasing adsorption energies on the three model surfaces.

Generally, the values obtained for crotonaldehyde and prenal on the two surface alloys are close to each other, being between ca. -222 and -235 kJ/mol (and up to -306 kJ/mol for η^4 forms) for the various flat configurations with dio(CC) and between -166 and -217 kJ/mol for those with π (CC) bonding at low coverages. For most corresponding cases, prenal interacts slightly weaker with the surface than crotonaldehyde (up to 10 kJ/mol), which implies, in conjunction with slightly higher surface deformation costs (also ca. 10 kJ/mol), that the weaker adsorption energies originate primarily from the higher steric demand.

The effect of alloying on the interaction energies of the flat η^2 , η^3 , and η^4 configurations is a slight weakening of less than 10% from Pt(111) to Pt₂Sn(111). For crotonaldehyde, the values decrease on average from ca. -241 kJ/mol on Pt(111), to ca. -229 kJ/mol on Pt₃Sn and ca. -220 kJ/mol on Pt₂Sn. The values for prenal change from -239 kJ/mol on Pt(111) to -245 kJ/mol on Pt₃Sn and ca. -208 kJ/mol on Pt₂Sn, respectively. The apparent increase of the average value to -245 kJ/mol for prenal on Pt₃Sn results mainly from the instability of the η^2 -dio(CC)-(s)-cis form there, which lowers the corresponding averages for crotonaldehyde. Moreover, due to increased

molecule and surface deformation costs, the interaction energies of the two η^4 prenol structures are quite large on Pt₃Sn(111).

Unfortunately neither the interaction energy nor the relaxation costs of surface and molecule seemed to exhibit a simple linear trend as a function of the Sn fraction. Both depend strongly on the bonding configuration. The surface deformation energies increase sizably with the Sn content, while the molecule distortion costs become only marginally larger due to an enhanced Pauli repulsion. Combined with the slight decrease of the interaction energies on the surface alloys, we therefore conclude that preferential destabilization of flat adsorption modes on the Pt–Sn surfaces, especially on Pt₂Sn, arises primarily from the increased surface deformation energies. Although the changes induced by the alloying on each of the three energy contributions are small, their balance, i.e., the adsorption energy, is affected sufficiently to induce the hapticity changes as detected with HREELS. Significantly larger interaction terms would be necessary to turn the high-hapticity structures of prenol into forms that would be competitive with the η^1 -top-OSn structures on the surface alloys.

4. Conclusions

We carried out studies aiming at the elucidation of the effects of alloying on adsorption and bonding of crotonaldehyde and prenol on Pt(111) and two Pt–Sn surface alloys. By combining HREELS and DFT, we obtained a detailed picture of the surface interaction and alloying effects at the atomistic level.

The presence of Sn dramatically simplifies the number of stable adsorption forms and reduces the adsorption energies strongly by ~20–30% for prenol and even 40–50% for crotonaldehyde from the values computed on Pt(111). Oxygen–tin bonds are required on the surface alloys in order to form sizably stable adsorption structures for the η^1 , η^3 , or η^4 coordination types. Flat structures such as the η^3 and η^4 forms are destabilized preferentially by Sn, thereby leading to less complex HREEL spectra on the surface alloys.

From the energy decomposition analysis, we find that variations of the adsorption energy on Pt(111), Pt₃Sn, and Pt₂Sn are primarily due to varying relaxation of the metal atoms in the adsorption complexes, i.e., elastic properties of the substrates. This is in line with the findings that we made simultaneously for the adsorption of small alkenes on these surfaces.^{48,49} Changes in the electronic effects caused by the alloying influence the bonding only to a lesser degree as evidenced from the similarities of the internal geometry parameters of the molecules in the adsorption complexes.

The interaction energies between the α,β -unsaturated aldehydes and the three surfaces decrease on average only by ~10% by alloying the Pt(111) substrate with Sn for a given coordination type. This is consistent with the small changes of vibrational frequencies of corresponding structures found with DFT and HREELS. Importantly, also the correlation of vibrational frequencies and shifts of groups involved in surface bonding with the adsorption energies is unsatisfying for these molecules, but invoking the interaction energies, the trends can be understood and support each other mutually.

The moderate lowering of the d-band center by alloying with Sn,²⁶ therefore, appears to be better in line with the moderate decrease of the interaction energy E_{int} rather than with the strong lowering of the adsorption energies E_{ads} , to which it is usually correlated.⁴⁶ Unlike in the case of simple adsorbates such as CO, where the interaction energy (bond strength) and the adsorption energy are closely related, these two properties are

different for multifunctional molecules interacting with a substrate in complex manners.

The deformation costs of the molecule and the surface reflect the relaxation of both geometries to form optimal adsorption configurations. The molecule deformation costs are usually dominating and depend mainly on the coordination type. They range from as little as 10 and 50 kJ/mol for the η^1 and η^2 - π (CC) forms to values between ~105 and ~316 kJ/mol for the high-hapticity η^3 -di σ (CC), η^4 - π (CC), and η^4 -di σ (CC) structures and are slightly larger (~10–23 kJ/mol) for prenol due to increased Pauli repulsions with the surface. Due to alloying, they increase from an average of ~18 and ~23 kJ/mol on pure Pt to ~37 and ~49 kJ/mol on Pt₃Sn and ~51 and ~61 kJ/mol on Pt₂Sn for the flat forms of crotonaldehyde and prenol. The increase is correlated to significantly larger outward relaxations on the surface atoms, as well as in-plane relaxations on Pt₂Sn(111).

The balance of slightly weaker interaction terms together with the increase in the surface deformation energies leads ultimately to the decrease in the adsorption energies and allows one to rationalize the change of coordination from flat η^2 , η^3 , and η^4 forms on Pt(111) to η^1 and η^2 structures on the Pt–Sn surfaces. For prenol, the energy balance on the surface alloys is no longer in favor of flat coordination types.

In summary, this study shows that a joint experimental and theoretical approach provides an atomic scale understanding of the vibrational and bonding properties of the adsorbed complex molecules. Particularly the vibrational properties of adsorbates can be better understood from the interaction energies rather than the adsorption energies. Often controversial topics such as the alloying effects or the changes correlated with different substitution patterns may be addressed successfully by this strategy.

Acknowledgment. We acknowledge funding by a bilateral CNRS-DFG project. J.H. thanks the Fonds der Chemischen Industrie for the scholarship grant.

References and Notes

- (1) Augustine, R. L. *Heterogenous Catalysis for the Synthetic Chemists*; Dekker: New York, 1996.
- (2) Bartok, M.; Felföldi, K. *Stereochemistry of Heterogeneous Metal Catalysts*; Wiley: Chichester, 1985; Chapter VII.
- (3) Common Fragrance and Flavor Materials; Wiley VCH: New York, 1985.
- (4) Jenck, J.; Germain, J. E. *J. Catal.* **1980**, *65*, 133.
- (5) Jerdev, D. I.; Olivas, A.; Koel, B. E. *J. Catal.* **2002**, *205*, 278.
- (6) Beccat, J.; Bertolini, J. C.; Gauthier, Y.; Massardier, J.; Ruiz, P. *J. Catal.* **1990**, *126*, 451.
- (7) Birchem, T.; Pradier, C. M.; Berthier, Y.; Cordier, G. *J. Catal.* **1996**, *161*, 68.
- (8) Borgna, A.; Anderson, B. G.; Saib, A. M.; Bluhm, H.; Hävecker, M.; Knop-Gericke, A.; Kuiper, A. E. T.; Tamminga, Y.; Niemantsverdriet, J. W. *J. Phys. Chem. B* **2004**, *108*, 17905.
- (9) Marinelli, T. B. L. W.; Naubuurs, S.; Ponec, V. *J. Catal.* **1995**, *151*, 431.
- (10) Marinelli, T. B. L. W.; Ponec, V. *J. Catal.* **1995**, *156*, 51.
- (11) Niemantsverdriet, J. W. *Spectroscopy in Catalysis*, 2nd ed.; Wiley-VCH: Weinheim, Germany, 2000.
- (12) Bent, B. E. *Chem. Rev.* **1996**, *96*, 1361.
- (13) Ibach, H.; Hopster, H.; Sexton, B. *Appl. Surf. Sci.* **1977**, *1*.
- (14) Ibach, H.; Mills, D. L. *Electronic Energy Loss Spectroscopy and Surface Vibrations*; Academic Press: New York, 1982.
- (15) Norskov, J. K.; Bligaard, T.; Logadottir, A.; Bahn, S.; Hansen, L. B.; Bollinger, M.; Bengaard, H.; Hammer, B.; Slijivancanin, Z.; Mavrikakis, M.; Xu, Y.; Dahl, S.; Jacobsen, C. J. H. *J. Catal.* **2002**, *209*, 275.
- (16) Chianelli, R. R.; Berhault, G.; Raybaud, P.; Kasztelan, S.; Hafner, J.; Toulhoat, H. *Appl. Catal., A* **2002**, *227*, 83.
- (17) Sabatier, P. *Ber. Dtsch. Chem. Ges.* **1911**, *44*.
- (18) Atrei, A.; Bardi, U.; Wu, J. X.; Zanazzi, E.; Rovida, G. *Surf. Sci.* **1993**, *290*, 286.

- (19) Batzill, M.; Beck, D. E.; Koel, B. E. *Surf. Sci.* **2000**, *466*, L821.
(20) Haubrich, J.; Loffreda, D.; Delbecq, F.; Sautet, P.; Jugnet, Y.; Krupski, A.; Becker, C.; Wandelt, K. *J. Phys. Chem. C* **2008**, *112*, 3701.
(21) Janin, E.; Schenck, H.; Ringler, S.; Weissenrieder, J.; Åkermark, T.; Göthelid, M. *J. Catal.* **2003**, *215*, 245.
(22) Paffett, M. T.; Windham, R. G. *Surf. Sci.* **1989**, *208*, 34.
(23) Paffett, M. T.; Gebhard, S. C.; Windham, R. G.; Koel, B. E. *Surf. Sci.* **1989**, *223*, 449.
(24) Birchem, T.; Pradier, C. M.; Berthier, Y.; Cordier, G. *J. Catal.* **1994**, *146*, 503.
(25) Delbecq, F.; Sautet, P. *J. Catal.* **2002**, *211*, 398.
(26) Delbecq, F.; Sautet, P. *J. Catal.* **2003**, *220*, 115.
(27) Delbecq, F.; Sautet, P. *J. Catal.* **1995**, *152*, 217.
(28) Hirschl, R.; Delbecq, F.; Sautet, P.; Hafner, J. *J. Catal.* **2003**, *217*, 354.
(29) Janin, E.; Ringler, S.; Weissenrieder, J.; Åkermark, T.; Karlsson, U. O.; Göthelid, M.; Nordlund, D.; Ogasawara, H. *Surf. Sci.* **2001**, *482*, 83.
(30) de Jesús, J. C.; Zaera, F. *Surf. Sci.* **1999**, *430*, 99.
(31) Loffreda, D.; Jugnet, Y.; Delbecq, F.; Bertolini, J. C.; Sautet, P. *J. Phys. Chem. B* **2004**, *108*, 9085.
(32) Loffreda, D.; Delbecq, F.; Vigne, F.; Sautet, P. *Angew. Chem., Int. Ed.* **2005**, *44*, 5279.
(33) Loffreda, D.; Delbecq, F.; Vigne, F.; Sautet, P. *J. Am. Chem. Soc.* **2006**, *128*, 1316.
(34) Murillo, L. E.; Chen, J. G. *Surf. Sci.* **2008**, *602*, 919.
(35) Haubrich, J.; Loffreda, D.; Delbecq, F.; Jugnet, Y.; Sautet, P.; Krupski, A.; Becker, C.; Wandelt, K. *Chem. Phys. Lett.* **2006**, *433*, 188.
(36) Haubrich, J.; Loffreda, D.; Delbecq, F.; Sautet, P.; Krupski, A.; Becker, C.; Wandelt, K. *J. Phys. Chem. C* **2009**, *113*, 13947.
(37) Loffreda, D.; Delbecq, F.; Sautet, P. *Chem. Phys. Lett.* **2005**, *405*, 38.
(38) Hoffman, R. *Rev. Mod. Phys.* **1988**, *60*, 601.
(39) Kresse, G.; Hafner, J. *Phys. Rev. B* **1993**, *47*, 558.
(40) Kresse, G.; Hafner, J. *Phys. Rev. B* **1993**, *48*, 13115.
(41) Perdew, J. P.; Wang, Y. *Phys. Rev. B* **1992**, *45*, 13244.
(42) Kresse, G.; Joubert, D. *Phys. Rev. B* **1999**, *59*, 1758.
(43) Neugebauer, J.; Scheffler, M. *Phys. Rev. B* **1992**, *46*, 16067.
(44) Delbecq, F.; Sautet, P. *Catal. Lett.* **1994**, *28*, 89.
(45) Morin, C.; Simon, D.; Sautet, P. *J. Phys. Chem. B* **2003**, *107*, 2995.
(46) Hammer, B.; Nørskov, J. K. *Adv. Catal.* **2000**, *45*, 71.
(47) Sachtler, W. M. *Vide* **1973**, *164*, 67.
(48) Becker, C.; Haubrich, J.; Wandelt, K.; Delbecq, F.; Loffreda, D.; Sautet, P. *J. Phys. Chem. C* **2008**, *112*, 14693.
(49) Haubrich, J.; Becker, C.; Wandelt, K. *Surf. Sci.* **2009**, *603*, 1476.

JP908353P